Optics Communications 283 (2010) 2102–2108

Contents lists available at ScienceDirect

Optics Communications

journal homepage: www.elsevier.com/locate/optcom

Unusual transmission through usual one-dimensional photonic crystal in the presence of evanescent wave

Yun-tuan Fang [a,*], Zhong-cheng Liang [b]

[a] Department of Physics, Zhenjiang Watercraft College, Zhenjiang 212003, China
[b] College of Optoelectronic Engineering, Center of Optofluidic Technology, Nanjing University of Posts and Telecommunications, Nanjing 210003, China

ARTICLE INFO

Article history:
Received 19 August 2009
Received in revised form 8 January 2010
Accepted 10 January 2010

ABSTRACT

Basing on the condition that the incident angle is larger than the total internal reflection angle, we present a systematic study of transmission properties of one-dimensional photonic crystal with all dielectric materials by the transfer matrix method and the Bloch's theorem. Due to the existence of the evanescent field within the structure, the transmission bands consist of some discrete symmetry peaks. For light with these peak frequencies, the structure is either transparent or opaque depending on the number of the structure periods. The unusual transmission properties are attributed to the field distribution and Bloch wave vector.

1. Introduction

Photonic crystals (PCs) have both fundamental interest and potential applications because of their unique ability to control and manipulate light [1–7]. A band diagram describes properties of an infinite periodic structure. Usually, PCs are composed of dielectric layers. But one-dimensional (1D) PCs composed of alternating layers of metal and dielectric materials [8–10] have some promising features, e.g. a 100% transmission of the evanescent waves is achieved by means of surface plasmon excitation [11,12]. However, Refs. [11,12] did not consider the effect of the loss of metal on the transmission of M-D PCs. If the loss of metal is considered, the ideal performance of the M-D PCs may be hardly obtained in real application. In this paper, we study the transmission properties of 1D PCs composed of alternating layers of two dielectric materials. Unlike previous studies that all the waves in dielectric layers are propagating mode, our study in this paper is based on the case that the electromagnetic wave is made evanescent within one of two dielectric materials through a proper incidence condition. Thus some unusual transmissions will be found, which unlike not only the transparent band of the M-D PCs, but also conventional pass bands of 1D PC. For example, for a special frequency, the structure considered here can be made total transparent (100% transmission), or be made almost opaque just through adding one period into its structure or cutting off one period from its structure. Due to its total dielectric structure, the effect of loss of the materials can be neglected.

2. Structure and Bloch mode

The schematic of 1D PC is shown in Fig. 1. The air-dielectric multilayer stack $(AD)^N$ is placed between two prisms (the grey layer D is dielectric and the white layer A is the air $(n_A = 1)$). The prisms on the top and bottom of the PC are used to couple light into and out of the PC, respectively. When the light is incident normally on the top surface of the top prism, it will enter into the PC with an incidence angle θ. As we have known, as light propagates from optically denser medium to optically thinner medium, there is a total reflection angle called θ_0 here. Without loss of generality, the refractive index for both the prisms and the layer D is firstly assumed to be $n_D = 3.23$. According to the geometrical optics and Fig. 1, the incidence angles from the layers D to layers A are all θ. If $\theta > \theta_0 = \arcsin(1/3.23) = 0.3184$ rad, all the electromagnetic wave within layers A is evanescent mode, while if $\theta < \theta_0$, the electromagnetic wave in all layers is propagating mode. As is well known, an evanescent wave cannot propagate through a single dielectric layer. However, evanescent waves in metallodielectric photonic crystal can propagate through evanescent coupling of surface plasmons between interfaces of metal/dielectric layers [11,12]. This transmission mechanism can be looked as a coupled-plasmon-resonant-waveguide (CPRW). The CPRW is a special case of the coupled-resonator optical waveguide (CROW) proposed by Yariv et al. [13]. The field in this case decays exponentially both in dielectric and in metal, but is amplified at each metal–dielectric interface. For our current structure, on the condition of $\theta > \theta_0$, the electromagnetic waves within layers A are all evanescent. Thus each layer D may be looked as a resonator cavity. If there is a coupling of evanescent wave between two layers D, the whole

* Corresponding author.
E-mail address: fang_yt1965@sina.com (Y.-t. Fang).

0030-4018/$ - see front matter © 2010 Elsevier B.V. All rights reserved.
doi:10.1016/j.optcom.2010.01.014

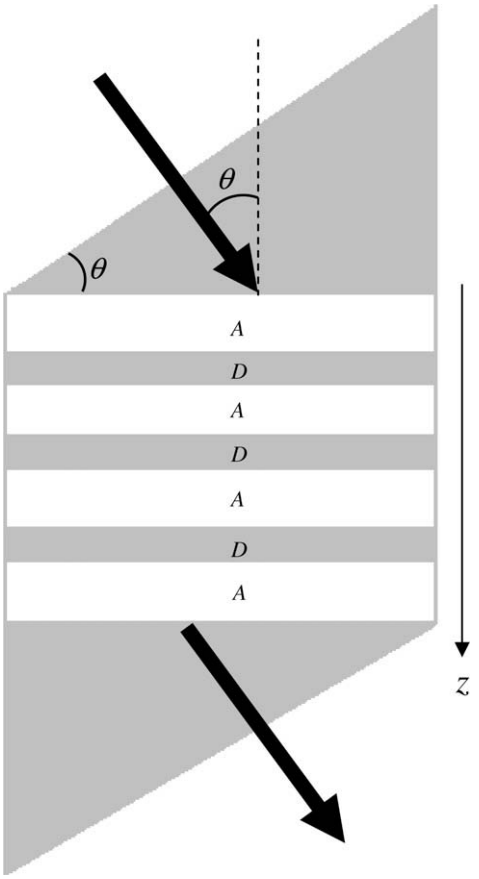

Fig. 1. Schematic of 1D PC.

structure can also be looked as a 1D analogy of the CROW. Thus a transmission wave-guiding may be achieved

Firstly, whether the infinite periodic structure of Fig. 1 has transmission band is dependent on the following dispersion equation derived from the Bloch's theorem [14]

$$\cos\beta_z(d_A+d_D)=\cos\left[k_z^{(A)}d_A\right]\cos\left[k_z^{(D)}d_D\right]-\frac{1}{2}\left(\frac{q_A}{q_D}+\frac{q_D}{q_A}\right)\times\sin\left[k_z^{(A)}d_A\right]\sin\left[k_z^{(D)}d_D\right] \quad (1)$$

where β_z is the z component of the Bloch wave vector, and $k_z^j=\omega/c\sqrt{\varepsilon_j}\sqrt{\mu_j}\cos(\theta_j)$ is the z component of wave vector $\boldsymbol{k}^j$ in the jth layer (c is light velocity in the vacuum and θ_j is the incident angle). d_A and d_D are the thicknesses of layers A and D, respectively. For TE wave, $q_j=\sqrt{\varepsilon_j}/\sqrt{\mu_j}\cos(\theta_j)$; for TM wave, $q_j=\sqrt{\mu_j}/\sqrt{\varepsilon_j}\cos(\theta_j)$. According to the geometrical optics, $\cos(\theta_A)=\sqrt{1-\sin^2(\theta)\times n_D^2}$, $\cos(\theta_D)=\cos(\theta)$. For $\theta>\theta_0$, $k_z^{(A)}$ is an imaginary quantity, $\cos[k_z^{(A)}d_A]=\cosh(|k_z^{(A)}d_A|)$, $\sin[k_z^{(A)}d_A]=i\times\sinh(|k_z^{(A)}d_A|)$. The condition of Eq. (1) having real solution for β_z is $|\cos\beta_z(d_a+d_b)|\leqslant 1$, which corresponds to the transmission band. The range of the transmission band corresponding to different incident angle and frequency can be calculated through Eq. (1). In the calculation, we let $\theta>0.32$ rad so that the wave from layers D enter into the layers A in evanescent mode. The results are shown in Fig. 2 from which the black area represents the transmission band at different layer thickness. The transmission wave within the transmission band is still Bloch mode. It is noted that for a fixed incident angle the frequency of transmission band decreases with d_D increasing, and the width of transmission band decreases with d_A increasing.

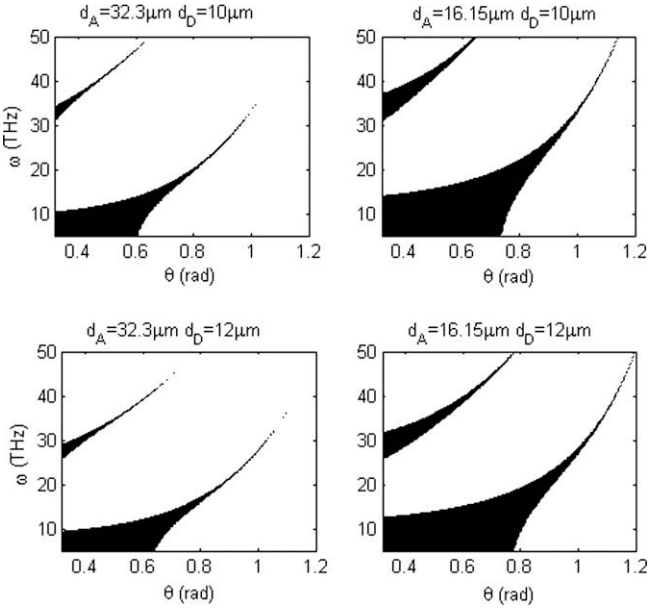

Fig. 2. Transmission band (black area) for different layer thicknesses.

3. Transmission properties of finite periodic structure

To further confirm the transmission of the Bloch waves, we apply a transfer matrix method to calculate the transmittance of a plane wave incident upon the structure with a finite number of periods. The plane wave is coupled into and out of the structure through two prisms. Although Fig. 2 is based on the infinite periodic structure, it still provides us a basis to analyze the finite structure. Without loss of generality, we fix $\theta=0.4$ rad and $d_A=32.3$ μm, $d_D=10$ μm. Because $\theta>\theta_0$, all the electromagnetic wave within layers A is evanescent mode. Fig. 3 shows the transmittance of TE wave for different period number. In order to compare the transmittance for $\theta>\theta_0$ with that for $\theta<\theta_0$, we also calculate the transmittance of TE wave for $\theta=0.2$ rad with different number of the periods. The result for $N=6$ is shown in Fig. 4. It is clear that there are clear differences between the transmission bands for $\theta>\theta_0$ and for $\theta<\theta_0$. For $\theta>\theta_0$, the transmission band consists of $N-1$ narrow transmission peaks. Except these transmission peaks, the transmittances at other frequencies are very small, even reach zero. Thus these transmission peaks are totally discrete. Through a detailed observation, we further find that the discrete transmission peaks for $\theta>\theta_0$ are centrosymmetric. Especially, for even period number, the position of the central peak does not change with increasing of the period number. However, for odd period number, all the positions of peaks change with increasing of the period number. Although the transmission features from Fig. 3 come from current structure parameters, through our studies, we find they can extend to other incidence angle for $\theta>\theta_0$. The property of the transmission band for $\theta>\theta_0$ can provide a new way to construct Dense Wavelength Division Multiplex (DWDM) filters for applications of telecommunications. The number and positions of filtering channels can be determined by the number of structure periods. Due to all dielectric materials, the loss of materials can be neglected, which make it has advantage over the M-D PCs in Ref. [11]. On the other hand, for $\theta<\theta_0$, there are also $N-1$ transmission peaks within the transmission band. But except these peaks, the transmittances at other frequencies are still large. Thus

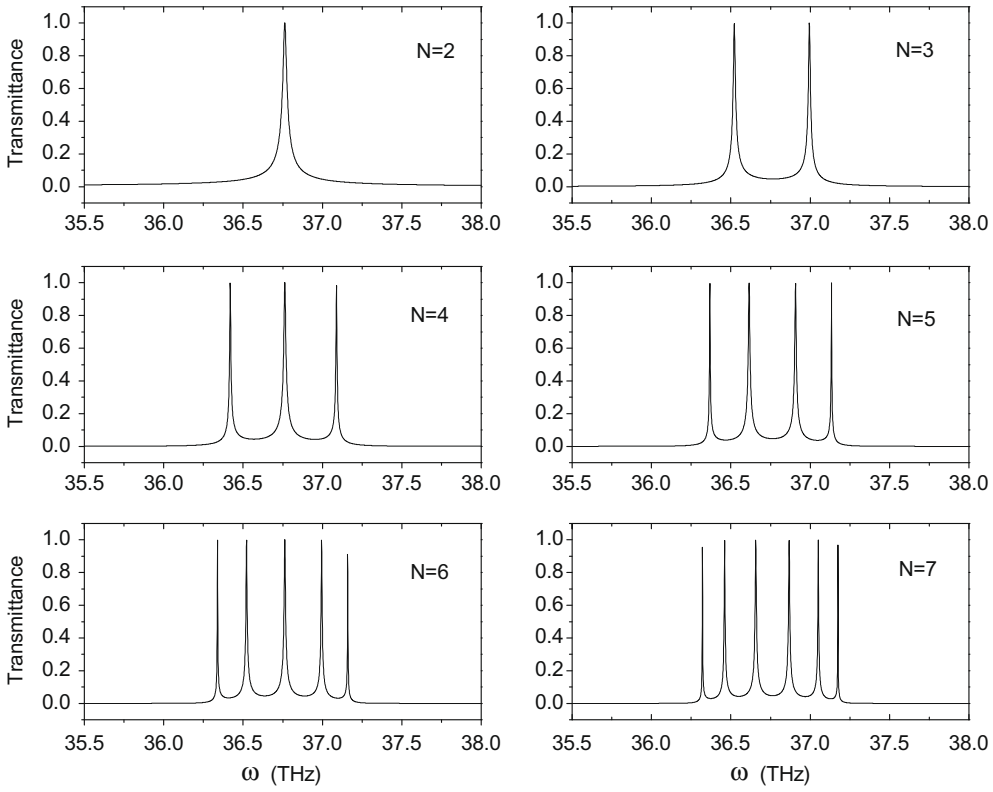

Fig. 3. The transmittance of TE wave for different number of periods. In the plots, $\theta = 0.4$ rad and $d_A = 32.3$ μm, $d_D = 10$ μm.

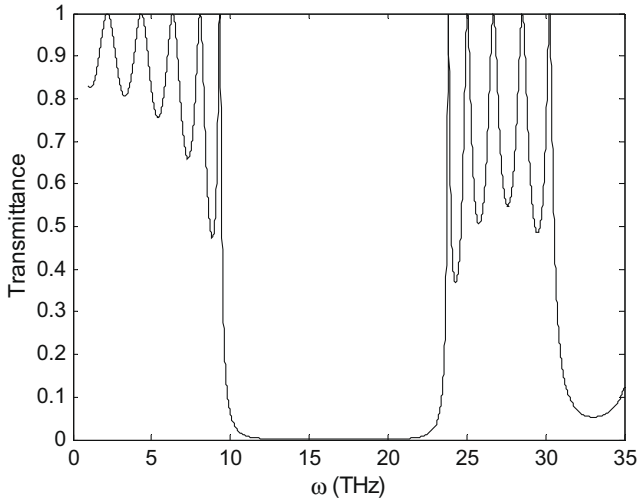

Fig. 4. The transmittance of TE wave for $\theta = 0.2$ rad and $N = 6$ ($d_A = 32.3$ μm, $d_D = 10$ μm).

these transmission peaks within the transmission band are not discrete.

Although the transmission properties for $\theta > \theta_0$ are much different from those for $\theta < \theta_0$, all the positions of transmission bands are still determined by Fig. 2 which corresponds to the Bloch mode for infinite periodic structure. The discrete resonance peaks within the transmission band is due to the coupling of cavity resonators through evanescent wave as we have indicated in Section 2. For the N-period structure, there are $N-1$ coupling, thus there are $N-1$ resonance peaks.

Up to here, the materials making up the structure are particular. However, the transmission properties for $\theta > \theta_0$ are general. As verification, we use SiO_2 make up the layer D and the two prisms ($n_D = 1.547$). The layer A is still composed of air in order to obtain large difference of refraction indexes. In this case, $\theta_0 = \arcsin(1/1.547) = 0.7029$ rad. Then we give the transmission spectra for $\theta = 0.8$ rad and $d_A = 20$ μm, $d_D = 10$ μm with different number of the periods in Fig. 5. The discrete narrow transmission peaks in Fig. 5 are similar to those in Fig. 3.

4. Effect of termination

Now we put attention on the central transmission peak at $\omega = 36.763$ THz for $\theta = 0.4$ rad and $N = 2$ in Fig. 3. Showing in

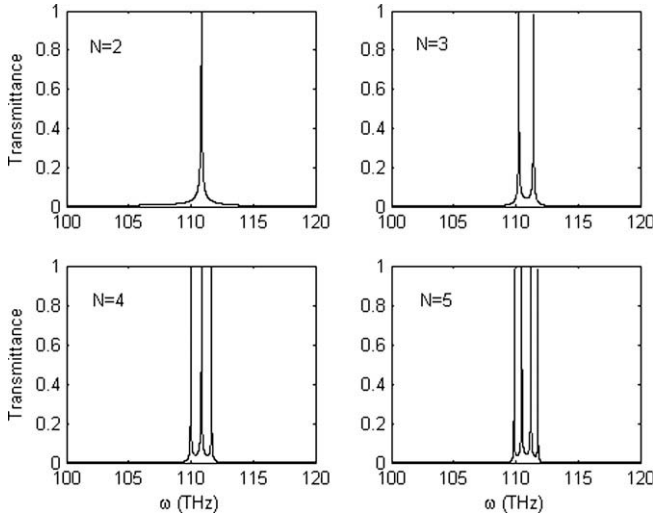

Fig. 5. The transmission spectra for $\theta = 0.8$ rad and $d_A = 20$ μm, $d_D = 10$ μm with different number of the periods. The layers A and D consist of air and SiO_2, respectively.

Fig. 6 (top plot) is the transmittance versus the number of the periods. The transmittance has only two values, which are either 1 for even number of the periods or 0.05 for odd number of the periods. The above rule of the transmittance can extend to arbitrary number of the periods. The strong dependence of transmittance on the number of periods only occurs for $\theta > \theta_0$. The striking result is that we can make this structure be either totally transparent or almost opaque only by adding one period into the structure or cutting off one period from the structure. We call it as the effect of termination. The direct reason for the effect of termination is that the position of the central peak does not change when the number of the periods increases with even number and the band structure is totally discrete. The physical reason is due to the resonance transmission. The small transmittance of 0.05 for odd number of the periods is because the resonance condition cannot be satisfied. But because the frequency is still within the transmission band, the transmittance has a small value and does not reach zero. In light of wave optics, due to the total internal reflection on the surface of layers *A*, there are *N* reflective beams. The two neighboring reflective beams have the same phase difference. For current frequency, the two neighboring reflective beams are just out of phase. Thus they with even number undergo destructive interference which leads to a perfect transmission. However, for odd number of the periods, there always exists one reflective beam that cannot be cancelled, which leads to an extraordinary low transmission.

The effect of termination is different from the transparent band as well as the nontransparent pass band in the M-D PCs [12]. The transparent band in the M-D structure allows 100% transmission independent of the thickness of the structure; while the nontransparent pass band in the M-D structure shows a wave-packet behavior with the thickness-dependent transmission. As we have indicated above, the effect of termination is only for $\theta > \theta_0$. For $\theta < \theta_0$, the effect disappears. In order to give a comparison, the bottom plot of Fig. 6 also shows the transmittance versus number of the periods for $\theta = 0.2$ rad at the frequency $\omega = 26.7$ THz which corresponds to the central peak within the second transmission band in Fig. 4. Although the transmittances reach 1 with even number of the periods, the minimal transmittances with odd number of the periods still overpass 0.5.

In order to obtain the detailed transmission properties for the condition of $\theta > \theta_0$, we still study the dependence of the transmittance on the number of the periods at the frequencies other than the central peak frequency. The structure and incidence angle are the same as Fig. 3. For reading convenience, in Fig. 3, we denote the peak frequency as ω_{N-k}, in which *N* indicates the period number, *k* is the order number of the peak (from left to right). For example, for $N = 4$, the three peak frequencies can be denoted as $\omega_{4-1} = 36.419$ THz, $\omega_{4-2} = 36.763$ THz and $\omega_{4-3} = 37.088$ THz. We firstly choose ω_{4-3} and ω_{6-4}. The results are shown in Fig. 7. For the top plot, the 100% transmission always occurs at $N = 4k$ (k is an integer number), and with other N ($N = 4k + 1$, $4k + 2$, $4k + 3$) the transmission keeps the minimal value, i.e., the transmittance changes with a period of $N = 4$. For the bottom plot, the 100% transmission always occurs at $N = 3k$, and with other N($N = 3k + 1$, $3k + 2$) the transmission keeps the minimal value, i.e., the transmittance changes with a period of $N = 3$. The results for ω_{4-1} and $\omega_{6-2} = 36.522$ THz are just the same as those for ω_{4-3} and ω_{6-4} due to the symmetry of the frequency spectra in Fig. 3 and are not plotted here. From Fig. 7, we find that the positions of some transmission peaks in Fig. 3 are the same for different *N*, for example, ω_{6-4} is equal to ω_{3-2}. It is noted from Fig. 7 that the effect of termination still occurs with some frequencies other than the central peak frequency.

5. Field distribution

Now, we study the electromagnetic field distribution and effective Bloch wave vector, which can help us further understand the transmission properties for $\theta > \theta_0$. The field distribution and effective Bloch wave vector can be obtained by transfer matrix method. In Fig. 8, we plot the electric field distributions with the same frequencies of incident light, incidence angles and structure parameters as those of Fig. 6 (top plot), Figs. 7 (top plot) and (bottom plot). The top plot, middle plot and bottom plot of Fig. 8 correspond to the frequencies $\omega_{2-1}, \omega_{4-3}$ and ω_{6-4}, respectively. The incident intensity at the first interface is supposed as 1 with no dimensionality.

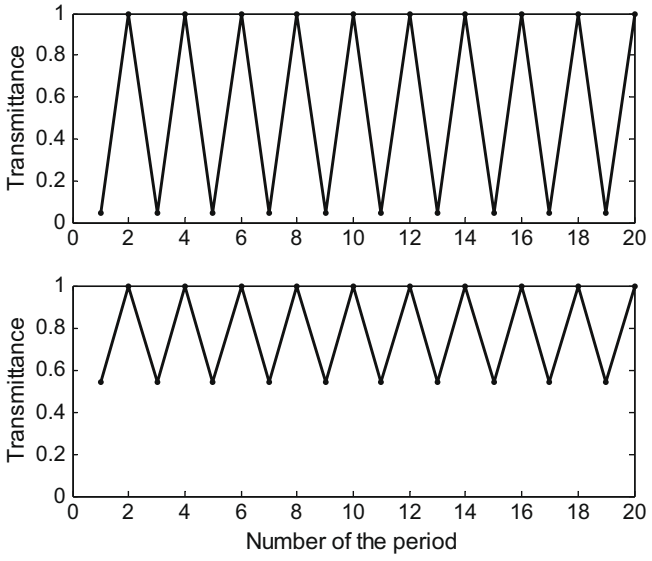

Fig. 6. The transmittance versus the number of periods for $\theta = 0.4$ rad, ω_{2-1} (top) and $\theta = 0.2$ rad, $\omega = 26.7$ THz (bottom) ($d_A = 32.3$ μm, $d_D = 10$ μm).

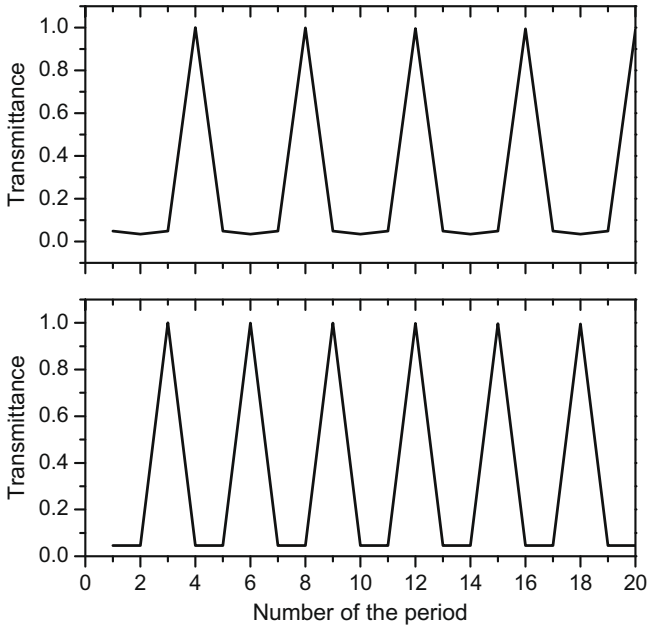

Fig. 7. The transmittance versus the number of periods for ω_{4-3} (top) and ω_{6-4} (bottom). Both the two frequencies correspond to the transmission peaks close to the central peak for $N = 4$ and $N = 6$ in Fig. 3, respectively. ($\theta = 0.4$ rad, $d_A = 32.3$ μm, $d_D = 10$ μm).

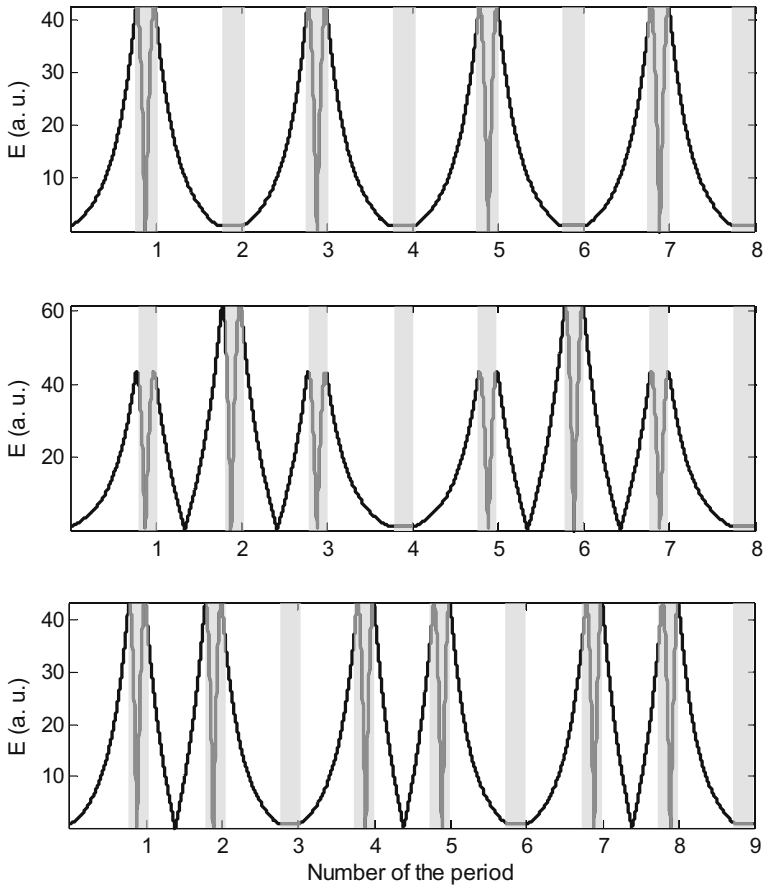

Fig. 8. The field distributions within the structure with different number of the periods for the frequencies ω_{2-1} (top), ω_{4-3} (middle) and ω_{6-4} (bottom). ($\theta = 0.4$ rad, $d_A = 32.3$ μm, $d_D = 10$ μm). The white area indicates the air layer and the grey area indicates dielectric layer.

The important common features of Fig. 8 are as follows: (i) All the field is localized at the interface of layers *A* and *D* and the field within all layers *A* decays or is amplified from the interface. (ii) The field periodically changes with the thickness increasing. The period of the field is two times of the structure period for ω_{2-1}, four times of the structure period for ω_{4-3}, three times of the structure period for ω_{6-4}, respectively. For ω_{4-1} and ω_{6-2}, the periods of the field are still the same as those ω_{4-3} and ω_{6-4}, respectively. The period of the field in Fig. 8 is just the same as the period of the transmittance in Figs. 6 and 7. (iii) Within the layer *D* connecting two field periods, the field always reaches the minimal value and keeps constant. Thus we can conclude that it is the period of the field that determines the period of the transmittance; and if the field pattern has no integer number of the period of the field, an ideal transmission cannot be obtained. This is verified by Fig. 9, in which the incidence frequency is the same as that of Fig. 8 (top plot), but the number of the period of structure changes from 8 to 7. As a result, the field pattern has 3.5 periods and the field intensity at the exit is much less than that at the entrance leading to a minimal transmission. Also the field distribution in Fig. 9 is different from that in Fig. 8. Thus for the finite structure, the field distribution is greatly dependent on the number of the period of structure. The result of Fig. 9 is also well agreement with that of Fig. 6 (top plot).

Up to now, we only consider the transmission properties within the transmission band basing on $\theta > \theta_0$. In this case, the major features are that the transmittance and the field distribution are much sensitive to the period number or the thickness of the structure. With the period number changing, there are only two cases: one is ideal transmission, the other is minimal transmission, and both the transmittance and the field periodically change. Next, we should consider the field distribution for the frequency within the band gap. Fig. 10 shows the field distribution with $\omega = 36$ THz for different period numbers. After a few periods, the field quickly decays to zero. Although both the transmittances for Figs. 9 and 10 are very small, the field distributions are totally different. In Fig. 9, the incident frequency is still within the transmission band and the field periodically changes with no decay through the whole structure, while in Fig. 10, the incident frequency is within the band gap and the field decays quickly with increasing period number.

6. Bloch wave vector

To better understand the physics behind all the above results, we analyze the Bloch wave vector. According to the Bloch's theorem, the amplitude of a wave inside PC structure must conform to the imposed periodicity. For current infinite 1D PC, the wave function can be described as

$$E(z) = u(z)\exp(i\beta_z z) \tag{2}$$

where $u(z+d) = u(z)$ $(d = d_A + d_D)$. Basing on Eq. (1), we calculate the value of β_z, the z component of Bloch wave vector for infinite structure. The structure parameters and incidence angle are the same as those of Fig. 3. Through some numerical calculations, we just obtain $\beta_z = 1/2\pi/d$ for ω_{2-1}; $\beta_z = 1/4\pi/d, 3/4\pi/d$ for ω_{4-3} and ω_{4-1}; $\beta_z = 1/3\pi/d, 2/3\pi/d$ for ω_{6-4} and ω_{6-2}; $\beta_z = 1 - 0.3105i\pi/d$ for $\omega = 36$THz, respectively.

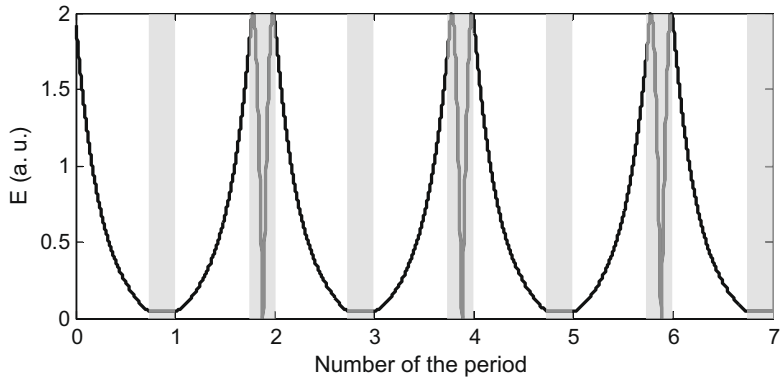

Fig. 9. The field distributions within the structure for ω_{2-1}, $N = 7$ and $\theta = 0.4$ rad($d_A = 32.3$ μm, $d_D = 10$ μm).

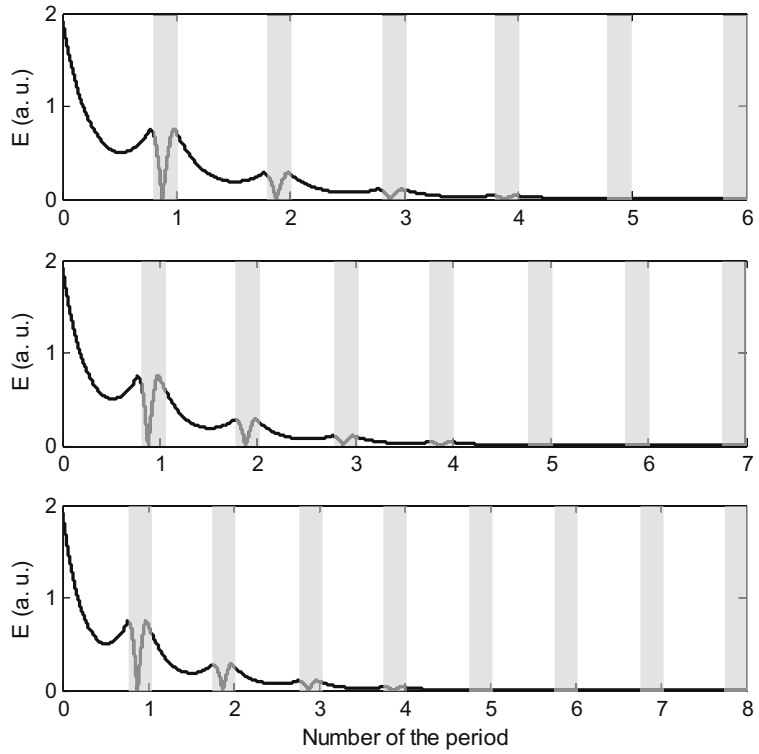

Fig. 10. The field distribution with $\omega = 36$ THz for different period number ($\theta = 0.4$ rad, $d_A = 32.3$ μm, $d_D = 10$ μm).

For $\beta_z = 1/2\pi/d$,

$$E(z+Nd) = u(z+Nd)\exp[i\beta_z(z+Nd)] = \pm u(z)\exp(i\beta_z z) = \pm E(z), \quad \text{if } N = 2k, \tag{3}$$

k is an integer number. (The period of field changing is $2d$).

Likely, for $\beta_z = 1/4\pi/d$ or $3/4\pi/d$,

$$E(z+Nd) = \pm E(z), \text{if } N = 4k. \text{ (The period of field changing is } 4d). \tag{4}$$

For $\beta_z = 1/3\pi/d$ or$2/3\pi/d$,

$$E(z+Nd) = \pm E(z), \text{if } N = 3k. \text{ (The period of field changing is } 3d) \tag{5}$$

In Figs. 5–8, all the transmittance and the field intensity are in absolute value. Thus Eqs. (3)–(5) well explain the changing period of the transmittance and the field. For the Bloch wave vector $\beta_z = 1 - 0.3105i$ for $\omega = 36$ THz with an imaginary quantity, the electromagnetic field decreases exponentially and is still modulated by the periodical function of $u(z)$, which also explain the result of Fig. 10.

We also calculate the values of β_z for other transmission peak frequencies in Fig. 3. An interesting and striking result has been found. For period number N, the values of β_z corresponding to peaks (from left to right) are just $(N-1)/N\pi/d, \ldots 2/N\pi/d$, $1/N\pi/d$ in turn. Thus we conclude that the transmittance and the field distribution periodically change with increasing structure periods for all transmission peak frequencies. The period of changing of the transmittance and the field distribution are dependent on both period number N and the position of transmission peak. For example, for $N = 10$ and the sixth transmission peak, $\beta_z = (10-6)/10\pi/d = 2/5\pi/d$, and the period of changing of the transmittance and the field distribution is five times of

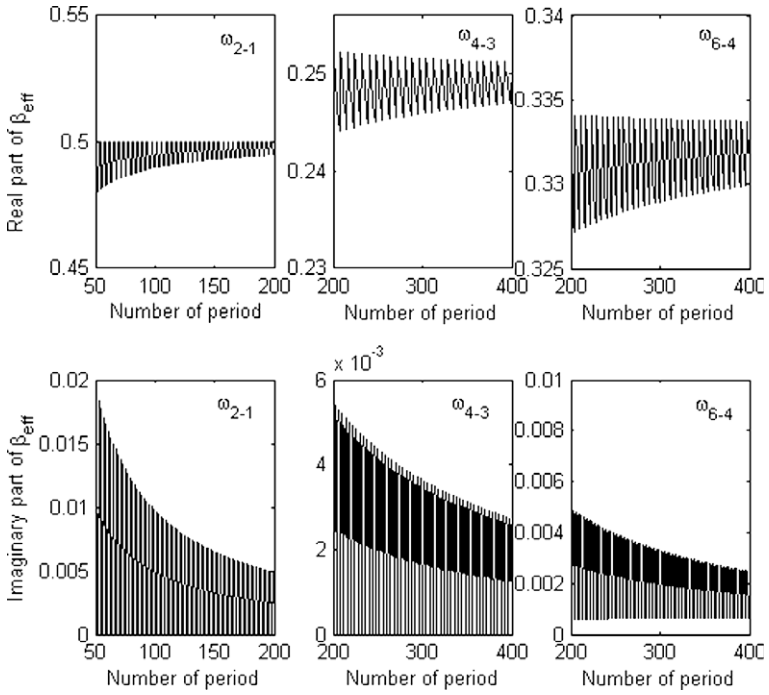

Fig. 11. The values of β_{eff} for ω_{2-1}, ω_{4-3} and ω_{6-4} ($\theta = 0.4$ rad, $d_A = 32.3$ μm, $d_D = 10$ μm).

structure period. We also perform calculations with other structures and incidence angles but keep $\theta > \theta_0$, and find the same conclusion.

The Bloch wave vector β_z is for infinite periodic structure. But for finite periodic structure, we can still use an effective Bloch wave vector β_{eff} to analyze the transmission properties. The concept of the effective Bloch wave vector is firstly defined through Ref. [15] and has been used to study the dispersion behavior of one-dimensional photonic crystals. According to Ref. [15], the effective Bloch wave vector is determined by

$$E_T = tE_I = \exp(i\beta_{eff}L)E_I \tag{6}$$

where E_T and E_I are the output intensity and the incident intensity, respectively. Thus the value of β_{eff} for current finite structure is determined by

$$t = \exp(i\beta_{eff}L) = |t|\exp(i\phi) \tag{7}$$

Where t is the transmittance with a complex value, L is the total thickness of the current structure and ϕ is the argument. For the same incidence angle $\theta = 0.4$ rad and structure parameters of $d_A = 32.3$ μm,$d_D = 10$ μm, the effective Bloch wave vector β_{eff} versus the number of the periods is shown in Fig. 11. The top plots show the real part of β_{eff}, the corresponding bottom plots shows the imaginary part of β_{eff}. It is clear that each real part of β_{eff} oscillates and the mean value gradually reaches but does not overpass the corresponding β_z with increasing number of the periods, while the imaginary part of β_{eff} are very small meaning the decay can be neglected. From Fig. 11, we find the finite length influences the value of β_{eff}, but β_z still determines the range of β_{eff}. Also, as the structure length extends to infinite, the real part of β_{eff} gradually reaches β_z, and the imaginary part of β_{eff} is close to zero.

7. Conclusions

In this paper, we have presented a detailed study of the transmission properties of 1D PC with all dielectric materials on the condition that the incident angle is larger than the total reflection angle. The existence of evanescent field within dielectric layers makes the 1D PC exhibit some unique properties which make it different from not only the M-D PCs but also 1D PC with all propagate mode. A termination effect is found. Unlike the M-D PCs, the loss is negligible due to all dielectric structure. These unusual transmission properties may provide a new means of controlling light in future optical device.

Acknowledgments

This work was supported by National Natural Science Foundation of China (Grant No. 60878037).

References

[1] E. Yablonovitch, Phys. Rev. Lett. 58 (1987) 2059.
[2] K.M. Ho, C.T. Chan, C.M. Soukoulis, Phys. Rev. Lett. 65 (1990) 3152.
[3] J.M. Bendickson, J.P. Dowling, M. Scalora, Phys. Rev. E 53 (1996) 4107.
[4] S. Olivier, C. Smith, M. Rattier, H. Benisty, C. Weisbuch, T. Krauss, R. Houdré, U. Oesterlé, Opt. Lett. 26 (2001) 1019.
[5] Y.-H. Ye, J. Ding, D.-Y. Jeong, I.C. Khoo, Q.M. Zhang, Phys. Rev. E 69 (2004) 056604.
[6] W.M. Robertson, J. Lightwave Technol. 17 (1999) 2013.
[7] J.M. Elson, K. Halterman, Opt. Express 12 (2004) 4855.
[8] V. Kuzmiak, A.A. Maradudin, F. Pincemin, Phys. Rev. B 50 (1994) 16835.
[9] M.M. Sigalas, C.T. Chan, K.M. Ho, C.M. Soukoulis, Phys. Rev. B 52 (1995) 11744.
[10] S. Fan, P.R. Villeneuve, J.D. Joannopoulos, Phys. Rev. B 54 (1996) 11245.
[11] Simin. Feng, J. Merle Elson, Pamela L. Overfelt, Opt. Express 13 (2005) 4113.
[12] Simin. Feng, J. Merle Elson, Pamela L. Overfelt, Phys. Rev. B 72 (2005) 085117.
[13] A. Yariv, Y. Xu, R.K. Lee, A. Scherer, Opt. Lett. 24 (1999) 711.
[14] A. Yariv, P. Yeh, Optical Waves in Crystals, Wiley, New York, 1984.
[15] S. Zhu, N. Liu, Z. Hang, H. Chen, Opt. Commun. 174 (2000) 139.